Clays and Clay Minerals, Vol. 66, No. 5, 449–465, 2018.

RELATING THE CATION EXCHANGE PROPERTIES OF THE BOOM CLAY (BELGIUM) TO MINERALOGY AND PORE-WATER CHEMISTRY

LANDER FREDERICKX[1,2,*], MIROSLAV HONTY[1], MIEKE DE CRAEN[1], REINER DOHRMANN[3], AND JAN ELSEN[2]

[1] Belgian Nuclear Research Centre (SCK·CEN), Boeretang 200, 2400 Mol, Belgium
[2] Department of Earth and Environmental Sciences, KU Leuven, Celestijnenlaan 200E, 3001 Leuven, Belgium
[3] BGR, Bundesanstalt für Geowissenschaften und Rohstoffe, Stilleweg 2, D-30655 Hannover, Germany

Abstract—The Boom Clay in northern Belgium has been studied intensively over recent decades as a potential host rock in the context of disposal of radioactive waste. One of the parameters of interest is the cation exchange capacity (CEC) as it is related to the sorption potential of radionuclides to the clay host rock. In the past, the CEC was determined using various methods on a limited number of samples, leading to significant variations. To constrain the CEC of the Boom Clay better, a sample set covering the entire stratigraphy was measured using the quick copper(II) triethylenetetramine method. Part of the sample set was also measured using the cobalt(III) hexamine method, as a quality control for the results of the former method. In addition, the exchangeable cation population of the Boom Clay was quantified systematically for the first time and these results were compared to the *in situ* pore-water chemistry, indicating a strong coupling between the pore-water composition and the exchangeable sites of clay minerals.

Key Words—Boom Clay, Cation Exchange Capacity, Clay Mineralogy, Pore Water.

INTRODUCTION

Due to the presence of heterovalent substitutions, most clay minerals possess a net negative charge, which allows for cations to be attracted to the surface of these minerals. The cation exchange capacity (CEC) is, therefore, a fundamental property of clay minerals and is defined as a measure of the ability of a soil to adsorb cations in such a form that they can be desorbed readily by competing ions (Bache, 1976). The CEC of a rock, according to Środoń and McCarty (2008), is the sum of the cations available for exchange held on the total specific surface area of the rock. As most heavy metals and radionuclides are cationic, clay minerals control, to a large extent, their adsorption behavior in the concepts of clays used as natural and engineered barriers for (radioactive) waste confinement (Dohrmann *et al.*, 2013).

The Boom Clay Formation in northern Belgium has been studied for decades as a potential host rock for the geologic disposal of radioactive waste. Various studies have been undertaken to determine the CEC of the Boom Clay (Baeyens *et al.*, 1985; Maes *et al.*, 2003; Fernandez *et al.*, 2010; Honty, 2010; Zeelmaekers *et al.*, 2015). Those studies applied different methodologies to determine the CEC (Table 1) with values ranging from 19.9 ± 3.1 cmol(+)/kg to 30.0 ± 3.9 cmol(+)/kg. The differences can be attributed to: (1) different methodologies used for the determination of the CEC; (2) a variable clay content in the studied sample sets; and (3) a lack of independent controls for the validity of the CEC data measured. The present study was performed in order to address these outstanding issues by: (1) using well established methodologies for CEC determination; (2) selecting a representative sample set covering the variability of the Boom Clay over the scale of the entire formation; and (3) verifying the CEC data measured using an independent control (quantitative mineralogical data).

In the present study, the CEC values of Boom Clay samples from the Mol site were determined by two techniques. The copper(II) triethylenetetramine method (Cu-trien) (Meier and Kahr, 1999; Ammann *et al.*, 2005) was applied, modified for Ca-bearing mineral phases after Dohrmann and Kaufhold (2009). The cobalt(III) hexamine (CoHex) method (Ciesielski *et al.*, 1997; ISO-23470, 2007; Dohrmann and Kaufhold, 2009) was applied as a reference method. By comparing the results of these two techniques with each other and with the results of previous studies, their validity for gauging the CEC can be estimated. Importantly, the accuracy of the results is tested by quantitative mineralogical data.

Other than the aforementioned issues, the exchangeable cation population has not yet been probed systematically in the Boom Clay. In the present study, a set of cation exchange population data of the Boom Clay is provided at various depth levels as determined by the two independent techniques. In addition, these data sets are compared to *in situ* pore-water compositions, which were sampled in the HADES Underground Research Facility (HADES URF) in the Boom Clay in Mol (Belgium) with the aid of piezometer filters. Although the pore-water composition has been the subject of a number of studies (*e.g.* Beaucaire *et al.* (2000) and De Craen *et al.* (2004a)), an in-depth comparison with

* E-mail address of corresponding author:
lander.frederickx@sckcen.be
DOI: 10.1346/CCMN.2018.064111

Table 1. Summary of average CEC values of Boom Clay samples reported in previous studies.

Borehole location	CEC (cmol(+)/kg)	# Samples	Ion exchanger	Reference
ON-Mol-1	20.4 ± 1.8	5	^{137}CsCl	Maes *et al.* (2003)
ON-Mol-1	19.9 ± 3.1	13	Cu-trien	Zeelmaekers *et al.* (2015)
HADES URF	30.0 ± 3.9	15	Ag-thiourea	Baeyens *et al.* (1985)
HADES URF	23.3 ± 3.1	3	$^{45}Ca(NO_3)_2$	Baeyens *et al.* (1985)
HADES URF	24.4 ± 3.4	5	$^{85}Sr(NO_3)_2$	Baeyens *et al.* (1985)
HADES URF	26.7 ± 2.5	4	$CsNO_3$	Fernandez *et al.* (2010)
HADES URF	21.8 ± 4.3	8	Cu-trien	Honty (2010)

cation exchange data has not yet been performed. In addition, the pore-water chemistry and the exchangeable cation population were used to calculate a range of selectivity coefficients, which can be compared to two sets of coefficients calculated by Baeyens *et al.* (1985) and De Craen *et al.* (2004a). Overall, the primary purpose of the approach adopted here was to assess the control of the mineralogy and pore-water chemistry on the CEC of the bulk clay and the composition of the cation exchange population on a formation scale.

MATERIALS AND METHODS

Materials

The main sample set of this study consisted of 20 Boom Clay samples from the ON-Mol-1 borehole drilled in 1997 at the SCK·CEN domain in Mol. The samples were preserved in vacuum-sealed Al-coated PE foil to prevent drying out, oxidation, and microbial alteration. One extra sample was taken during the excavation of the PRACLAY gallery in the HADES URF (Bastiaens *et al.*, 2008) and was preserved under similar conditions. In addition to these 21 samples, another 32 samples, left over from previous studies, were used to extend the dataset. The extended sample set consisted of 11 samples from the ON-Mol-1 borehole, originally reported by Zeelmaekers *et al.* (2015); 12 samples from the drilling of piezometer TD-11D, originally reported by De Craen *et al.* (2004b); and nine samples from the drilling of piezometer CG-13U, originally reported by De Craen (2005). These samples were preserved in a powdered and dried form. Sample names and provenance depths are shown in Tables 2 and 4.

Methods

The fresh samples of the main sample set were cut into cm-sized pieces and dried subsequently in an oven at 60ºC while being exposed to oxygen. After drying, the

Table 2. Results of the Cu-trien experiments for the main sample set. All values are indicated in cmol(+)/kg. The depths of each sample are reported in meters relative to the Belgian reference altitude (TAW).

Sample	Depth (mTAW)	CEC (Cu-VIS)	CEC (Cu-ICP)	Ca	K	Mg	Na	Sum	SO_4	Adjusted Ca	Adjusted Sum
ON-Mol-1-43b	−162.90	14.4	14.8	9.8	2.1	9.6	3.9	25.4	4.9	4.9	20.5
ON-Mol-1-60b	−179.70	17.7	17.9	9.9	2.4	5.3	5.7	23.3	2.4	7.5	20.9
ON-Mol-1-63b	−182.70	19.8	20.2	9.8	2.4	7.8	6.7	26.7	3.1	6.7	23.6
ON-Mol-1-67b	−186.60	22.4	21.8	6.5	2.8	5.0	8.2	22.5	0.6	5.9	21.9
ON-Mol-1-72b	−191.50	24.6	25.0	7.7	3.4	5.8	9.4	26.3	1.5	6.2	24.8
ON-Mol-1-73b	−192.50	24.0	24.3	7.0	3.3	6.1	9.3	25.7	1.4	5.6	24.3
ON-Mol-1-76b	−195.50	22.4	22.6	9.2	2.6	6.9	8.3	26.9	2.2	7.0	24.7
PRACLAY	−196.50	22.4	23.2	8.8	2.7	7.0	8.8	27.3	2.3	6.5	25.0
ON-Mol-1-78b	−197.50	22.3	22.4	7.6	3.0	6.6	8.9	26.1	2.3	5.3	23.8
ON-Mol-1-82c11	−201.30	21.9	21.3	6.4	2.6	7.2	8.7	24.9	1.7	4.7	23.2
ON-Mol-1-90c11	−208.90	25.7	25.9	6.7	3.3	6.4	11.2	27.6	1.6	5.1	26.0
ON-Mol-1-98c1	−216.90	18.8	18.5	4.1	2.3	5.7	8.1	20.2	1.3	2.8	18.9
ON-Mol-1-102a1	−221.30	22.0	23.1	2.5	3.4	10.4	10.4	26.7	2.5	0.0	24.2
ON-Mol-1-103b	−222.10	25.0	25.8	5.1	3.1	6.0	11.3	25.5	1.4	3.7	24.1
ON-Mol-1-108b	−227.10	23.2	23.5	8.2	2.7	6.1	10.4	27.5	2.3	5.9	25.2
ON-Mol-1-115b	−234.10	23.7	24.0	4.8	2.9	4.7	11.2	23.6	1.0	3.8	22.6
ON-Mol-1-119b	−238.0	16.2	16.6	4.6	2.1	5.8	7.6	20.0	2.3	2.3	17.7
ON-Mol-1-125b	−243.90	21.0	20.6	7.0	2.7	5.3	10.3	25.3	2.3	4.7	23.0
ON-Mol-1-130a2	−249.0	15.7	16.7	8.9	2.1	4.9	7.5	23.3	3.8	5.1	19.5
ON-Mol-1-131b	−250.0	19.1	19.3	11.2	2.5	4.8	8.9	27.4	4.0	7.2	23.4
ON-Mol-1-143b	−261.90	7.6	8.2	5.6	1.0	2.2	3.6	12.4	2.2	3.4	10.2

https://doi.org/10.1346/CCMN.2018.064111 Published online by Cambridge University Press

samples were split by coning and quartering into three fractions: one fraction for the application of the CoHex technique at the BGR in Hannover, one for the application of the Cu-trien technique, and one for the determination of the bulk-rock mineralogy by X-ray diffraction (XRD). The 32 samples of the extended sample set were only measured using the Cu-trien method due to limitations in remaining sample mass.

Cation exchange experiments. The samples used for the cation exchange experiments were oven dried at 60ºC. Duplicates of each sample were dried at 110ºC to determine the water loss. This information was used to recalculate the mass of each sample in the experiments to a dry mass at 110ºC. Note that the samples were exposed to oxygen prior to contact with Cu-trien and CoHex. This prevents the error described by Hadi *et al.* (2016) for CEC determination of clay under reducing conditions using CoHex.

CoHex measurements. The exchange solution was prepared as described by Dohrmann and Kaufhold (2009): 2 L of a 0.0166 M Co(III) hexamine solution (STREM Chemicals, Newburyport, Massachusetts, USA) was placed in a beaker, after which 2 g of fine-grained calcite was added in order to prevent the dissolution of carbonate minerals present in the samples. The mixture was placed in an ultrasonic bath for 30 min and then stirred for a further 30 min. Afterward, the remaining undissolved calcite was allowed to settle overnight. Then, 50.0 mL of this solution was added to centrifugation tubes containing 3 g or 5 g of sample. The tubes were placed in an end-over-end shaker for 2 h followed by centrifugation. The 2 mL of the supernatant was diluted using a HNO_3 solution, after which the exchangeable cations, the index cation, and sulfur were measured by inductively coupled plasma (ICP) analysis (ThermoScientific ICAP 6300 Duo ICP-OES, Waltham, Massachusetts, USA).

Cu-trien measurements. The exchange solution was prepared as described by Dohrmann and Kaufhold (2009): 2 L of a 0.01 M Cu-trien solution (VWR Chemicals, Leuven, Belgium) was placed in a beaker, after which the calcite (J.T. Baker, Center Valley, Pennsylvania, USA) saturation was applied exactly as in the previous paragraph. 50.0 mL of this solution was added to centrifugation tubes containing 2 g and 3 g of sample. The tubes were placed in a horizontal shaker overnight followed by centrifugation. 250 µL of the supernatant was diluted using 4.75 mL of deionized water, after which the exchangeable cations, the index cation, and sulfur were measured by ICP analysis (Varian 720-ES ICP-OES, Agilent, Santa Clara, California, USA). Another 3 mL of supernatant was used to determine the CEC by measurement of the extinction of the solution at 577 nm by photometric analysis (Lambda 40, Bodenseewerk Perkin Elmer, Uberlingen, Germany). Reference blank solutions were used both for the ICP and photometric analyses.

X-ray diffraction (XRD) analysis. For mineralogical characterization, XRD measurements were performed on randomly oriented powders. Samples were mixed with 10 wt.% of an internal standard (ZnO) and milled in a wet state for 5 min in a McCrone micronizing mill (Snellings *et al.*, 2010). After drying, the powder was side loaded into the measurement holders. The measurements were executed using a Philips PW1830 X-ray diffractometer in a Bragg-Brentano setup with CuKα radiation, a graphite monochromator, and a gas proportional detector. The operational parameters of the device were set at 45 kV and 30 mA from 5 to 65º2θ with a step size of 0.02º2θ and a 2 s scanning time per step. The quantitative mineralogical composition was determined by processing the measured XRD patterns using the *Quanta* software (© Chevron ETC).

To quantify the detailed clay mineralogy, the fraction of each <2 µm sample was separated by centrifugation after removal of aggregate-forming particles (after Jackson, 1975) and saturation with Ca. Oriented clay slides of these fractions were prepared and measured, using the same diffractometer, in both air-dried and ethylene glycolated states. The XRD patterns were then processed using the *Sybilla* clay-modeling software (© Chevron ETC).

The bulk mineralogical composition and the clay mineral composition were combined subsequently following the procedure described by Zeelmaekers *et al.* (2015) in order to obtain a quantitative speciation of clay minerals in the bulk rock.

Organic carbon analysis. As the Boom Clay contains non-crystalline organic compounds in addition to the phases probed by XRD, the total organic carbon (TOC) content was determined using a LECO CS-444 analyzer by heating powdered samples. The TOC in each sample was converted to a percentage of organic matter (OM) using a factor of 1.47, calculated from the H/C and O/C ratios in Boom Clay kerogen (Deniau *et al.*, 2008).

Pore-water analysis. Complementary to solid samples, geochemical data of the pore waters from the piezometer filters in the Boom Clay were used in order to test if the pore-water chemistry can be correlated with the cation occupancies at similar depths. The piezometers allow for *in situ* pore-water sampling, limiting the perturbations and artifacts necessarily related to pore-water acquisition. The pore waters were acquired from the vertical piezometers CG-13U, CG-13D, and TD-11D installed at the HADES-URF. Altogether, pore waters were sampled from various Boom Clay layers over a depth interval of 64 m. The porous filter screen of piezometer TD-11D is made from Schumatherm (Fluxa Filtri, Mazzo di Rho,

https://doi.org/10.1346/CCMN.2018.064111 Published online by Cambridge University Press

Italy) whereas stainless steel (AISI 316 L/B) was used for the construction of the filter screens of CG-13U and CG-13D. No important differences in the chemical composition of the pore waters were found between these piezometers despite the use of a range of materials (De Craen *et al.*, 2004a). The data of the last sampling campaign carried out in 2017, kindly made available by ONDRAF/NIRAS, were used for comparison with the CEC.

RESULTS

Cu-trien method

The CEC values (Tables 2, 4) determined by photometric analysis (CEC(Cu-VIS)) and those determined by ICP analysis (CEC(Cu-ICP)) show good agreement (Figure 1). These parameters show a high degree of correlation (R^2 = 0.94), with a systematic difference of 2% between them. Upon closer examination, the deviation is clearly due largely to the TD-11D and CG-13U sample sets, in which the deviation amounts to 5%. No significant deviation was found in the sample sets from the ON-Mol-1 borehole. As the TD-11D and CG-13U sample sets were stored in a powdered form for several years, subpar storage conditions clearly may have affected the outcome of the analyses.

The average CEC determined by photometric analysis for the entire sample set (n = 53) was 21.7 ± 3.3 cmol(+)/kg, while the average CEC determined by ICP analysis was 22.2 ± 3.3 cmol(+)/kg. These values are comparable to the average of 21.8 ± 4.3 cmol(+)/kg reported by Honty (2010) (CEC(Cu-VIS)) for a limited number of samples (n = 8). The isotopic dilution methods ($^{45}Ca(NO_3)_2$ and $^{85}Sr(NO_3)_2$) used by Baeyens *et al.* (1985) also yielded similar average values. Experiments with other exchange complexes (Table 1), such as $CsNO_3$ (Fernandez *et al.*, 2010) and Ag-thiourea (Baeyens *et al.*, 1985), yielded greater CEC values (26.7 ± 2.5 cmol(+)/kg and 31.0 ± 3.6 cmol(+)/kg, respectively). Problems with high Ag-thiourea CEC values in the presence of expandable clay minerals caused by excess adsorption of Ag-thiourea leading to unreliable CEC results dependent on the solution/solid ratio and the ionic strength of the exchange solution were reported by Dohrmann (2006). The high values reported by Baeyens *et al.* (1985) can be attributed to this process.

As demonstrated by the standard deviation, the CEC values vary throughout the Boom Clay stratigraphy. The CEC(Cu-ICP) values at the corresponding depths in the Boom Clay, next to a microstratigraphic log of the ON-Mol-1 borehole indicating the predominantly clay- (dark) and silt-sized (light) layers, are shown in

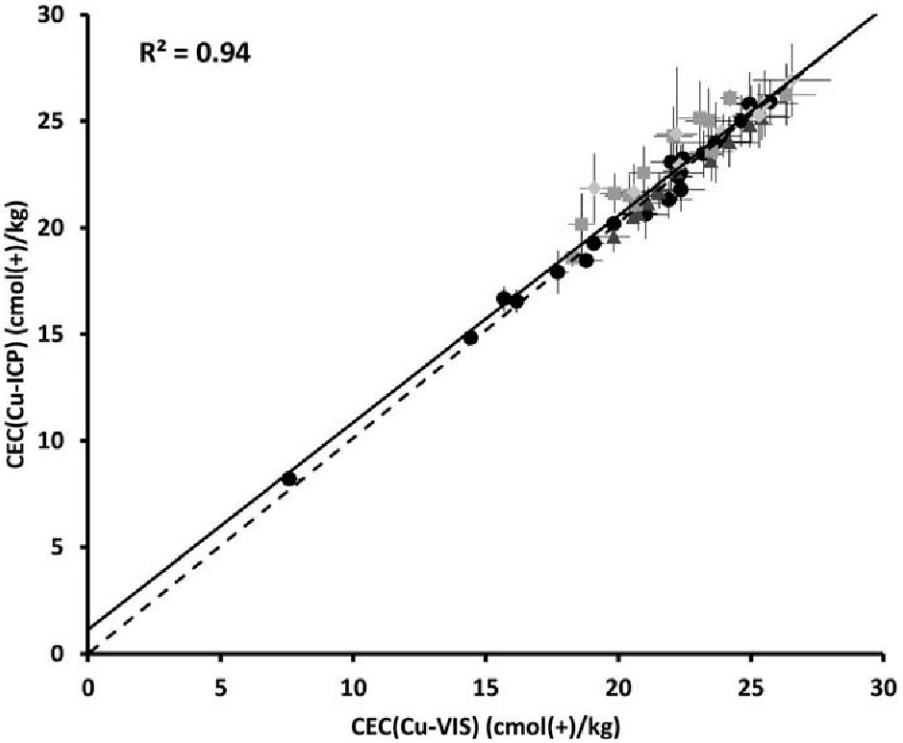

Figure 1. Comparison of the CEC values determined by ICP analysis and VIS-photometry. Standard deviations based on two measurements are indicated. The trend line (CEC(Cu-ICP) = 1.023CEC(Cu-VIS)) is indicated in black. Circles indicate the main sample set, triangles the set of Zeelmaekers *et al.* (2015), squares the set of De Craen *et al.* (2004b), and diamonds the set of De Craen (2005).

https://doi.org/10.1346/CCMN.2018.064111 Published online by Cambridge University Press

Figure 2. The predominantly silt-sized Boeretang Member has an average CEC(Cu-ICP) of 21.5 ± 3.6 cmol(+)/kg (n = 15). The relatively high standard deviation is reflected by the high degree of variation in lithology within the member. The Putte Member, in which the HADES URF is located, has the greatest CEC value (Cu-ICP) at an average of 22.9 ± 0.4 cmol(+)/kg (n = 26). The Terhagen Member has an average CEC(Cu-ICP) of 22.0 ± 0.6 cmol(+)/kg (n = 11) and the silt- to sand-dominated Belsele-Waas Member has an indicative CEC(Cu-ICP) of 8.2 cmol(+)/kg, although this is based on only one measurement at the base of the formation.

The exchangeable cation population (Tables 2 and 4) is made up of similar concentrations of Ca, Mg, and Na, with small contributions from K. The average population consists of 7.7 ± 2.4 cmol(+)/kg Ca, 6.6 ± 1.9 cmol(+)/kg Mg, 8.4 ± 1.9 cmol(+)/kg Na, and 3.2 ± 0.7 cmol(+)/kg K. On average, the sum of cations is 3.8 cmol(+)/kg more than the CEC(Cu-ICP).

CoHex method

The average CEC (Co-ICP) (Table 3) of the main sample set was 22.2 ± 5.0 cmol(+)/kg which is 1.5 cmol(+)/kg less than the average with the Cu-trien method. This discrepancy is acceptable as it falls in the same range as differences reported by Dohrmann and Kaufhold (2009) for two clay samples. The differences between the Cu-trien and CoHex technique seem to increase with increasing CEC (Figure 3, bottom right). A detailed study, covering a large range of CEC values, could shed more light on the details of this observation. Nevertheless, the correlation between the two techniques is strong (R^2 = 0.85, CEC(Cu-ICP) = 0.93.CEC(Co-ICP)).

The exchangeable cation population (Table 3) is similar to that determined by the Cu-trien method. At an average misfit of <5% little or no misfit was observed between the methods for Na and K (Figure 3). For Ca and Mg, the average misfit was between 5 and 10%. The values for SO_4 are, however, systematically ~30% less than the corresponding Cu-trien values. The shift can be attributed to the fact that the Cu-trien solution was prepared with $CuSO_4$, while the CoHex solution was sulfate free. Small concentrations of sulfate released into the solution during the exchange experiment were, therefore, detected more reliably in a sulfate-free CoHex solution. Consequently, the observed errors (Figure 3) were smaller for the CoHex method, which indicates that the SO_4 inventory derived with this method is more reliable.

Pore-water chemistry

The concentrations of the major exchangeable cations of the Boom Clay pore waters sampled in 2017 are plotted in Figure 4. Pore-water data from filters located in the

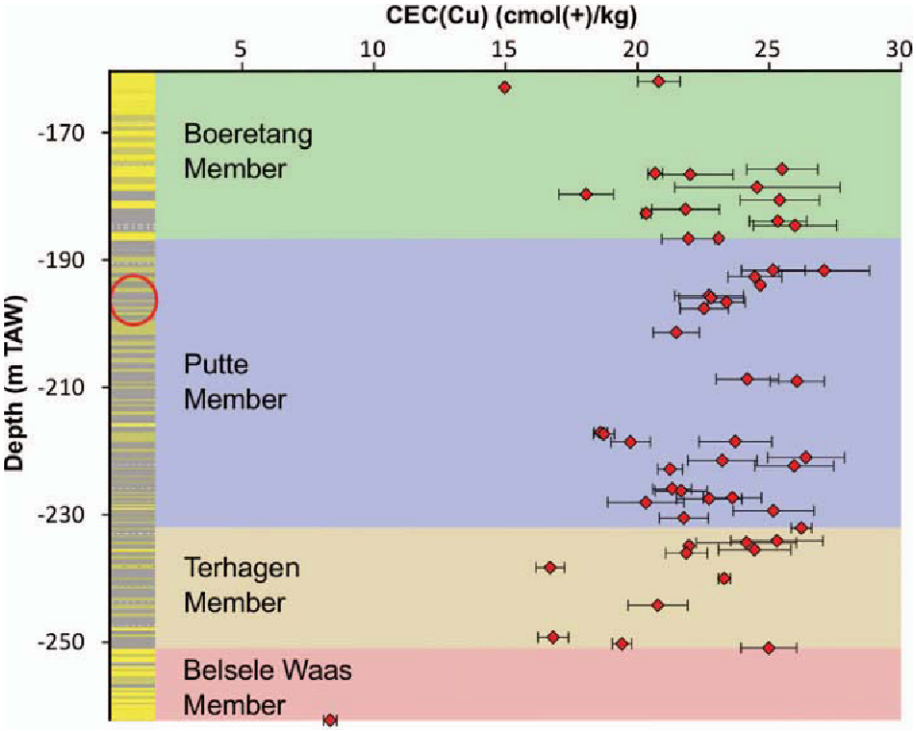

Figure 2. CEC of the sample set throughout the Boom Clay stratigraphy. A stratigraphic column (Vandenberghe *et al*., 2014), with increasing lightness for increasingly coarse layers, is indicated on the left. The HADES URF is indicated by the larger circle to the left of the image. Standard deviations, based on two measurements, are indicated by the error bars.

https://doi.org/10.1346/CCMN.2018.064111 Published online by Cambridge University Press

Table 3. Results of the CoHex experiments for the main sample set. All values are indicated in cmol(+)/kg.

Sample	CEC (Co-ICP)	Ca	K	Mg	Na	Sum	SO_4	Adjusted Ca	Adjusted Sum
ON-Mol-1-43b	13.8	9.9	1.9	11.0	4.2	26.9	4.8	5.1	22.1
ON-Mol-1-60b	19.7	9.1	2.3	6.0	6.3	23.6	1.5	7.6	22.1
ON-Mol-1-63b	21.3	12.3	2.4	8.5	6.8	29.9	3.0	9.3	26.9
ON-Mol-1-67b	25.4	7.7	2.9	5.5	8.5	24.6	0.4	7.3	24.2
ON-Mol-1-72b	26.4	7.4	3.4	5.9	9.8	26.4	0.8	6.6	25.6
ON-Mol-1-73b	26.5	7.8	3.1	6.9	9.5	27.2	1.1	6.7	26.1
ON-Mol-1-76b	28.1	11.7	2.4	8.3	8.6	30.9	1.9	9.8	29.0
PRACLAY	25.1	10.1	2.9	8.3	9.1	30.4	1.6	8.5	28.8
ON-Mol-1-78b	25.2	8.8	2.9	8.2	9.2	29.1	2.1	6.7	27.0
ON-Mol-1-82c11	26.1	6.7	2.7	7.3	9.4	26.0	0.8	5.9	25.2
ON-Mol-1-90c11	28.7	7.3	3.1	7.0	11.4	28.7	0.8	6.5	27.9
ON-Mol-1-98c1	20.3	4.4	2.5	6.1	8.8	21.7	1.1	3.3	20.6
ON-Mol-1-102a1	22.7	4.2	2.9	10.8	10.2	28.0	2.7	1.5	25.3
ON-Mol-1-103b	26.2	5.4	3.0	7.0	11.6	26.9	1.0	4.4	25.9
ON-Mol-1-108b	25.2	8.8	2.6	6.8	10.7	28.8	1.9	6.9	26.9
ON-Mol-1-115b	21.6	4.6	2.6	4.5	10.4	22.0	0.4	4.2	21.6
ON-Mol-1-119b	17.6	3.9	2.1	5.6	8.2	19.7	1.5	2.4	18.2
ON-Mol-1-125b	21.0	6.8	2.2	5.1	9.7	23.7	1.2	5.6	22.5
ON-Mol-1-130a2	17.8	10.3	2.2	5.9	8.6	27.0	3.5	6.8	23.5
ON-Mol-1-131b	19.4	12.3	2.4	5.0	9.2	28.8	3.4	8.9	25.4
ON-Mol-1-143b	8.4	4.7	1.2	2.6	4.1	12.5	1.5	3.2	11.0

Table 4. Results of the Cu-trien experiments for the extended sample set. All values are indicated in cmol(+)/kg. The depth of each sample is reported in meters relative to the Belgian reference altitude (TAW).

Sample	Depth (mTAW)	CEC (Cu-VIS)	CEC (Cu-ICP)	Ca	K	Mg	Na	Sum	Adjusted Ca	Adjusted Sum
ON-Mol-1-42a	−162	20.8	20.7	8.4	3.1	9.6	5.1	26.2	5.9	23.7
ON-Mol-1-57c12	−176.3	20.6	20.5	10.5	2.8	5.7	6.4	25.4	8.6	23.5
ON-Mol-1-65c2	−183.9	25.4	25.2	13.1	3.7	10.6	9.0	36.4	8.8	32.1
ON-Mol-1-77c122	−195.9	22.2	22.6	14.7	3.1	6.6	8.7	33.1	10.9	29.3
ON-Mol-1-90c2	−208.6	24.2	24.0	12.2	3.4	7.2	10.6	33.4	8.8	30.0
ON-Mol-1-100c2	−218.4	19.8	19.6	7.1	2.8	11.7	9.6	31.2	1.7	25.8
ON-Mol-1-107c21	−225.7	21.1	21.2	8.2	2.7	8.7	9.6	29.2	4.6	25.6
ON-Mol-1-116c21	−234.6	21.5	21.8	6.8	3.0	9.9	10.0	29.7	3.4	26.3
ON-Mol-1-118c	−235.8	21.5	21.7	4.6	3.0	5.8	10.2	23.6	3.1	22.1
ON-Mol-1-121c1	−239.7	23.5	23.1	10.7	2.7	9.2	9.6	34.1	4.3	27.7
ON-Mol-1-132c21	−250.6	25.0	24.8	7.2	3.6	4.7	11.6	27.1	5.7	25.6
TD-11D-217.1	−217.1	18.3	18.6	4.5	2.7	5.9	7.8	20.9	3.2	19.6
TD-11D-218.3	−218.3	23.5	23.6	5.8	3.1	8.2	9.7	26.8	3.7	24.7
TD-11D-220.8	−220.8	26.3	26.2	6.2	4.1	7.7	11.1	29.1	4.4	27.3
TD-11D-222.6	−222.6	20.7	21.1	6.5	3.4	8.4	8.7	27.0	3.9	24.4
TD-11D-226	−226	20.4	21.5	7.3	3.2	6.3	8.3	25.1	5.6	23.4
TD-11D-227.2	−227.2	21.0	22.6	7.7	3.0	5.0	8.7	24.4	6.8	23.5
TD-11D-227.8	−227.8	18.6	20.2	8.6	2.9	4.5	7.5	23.6	7.2	22.2
TD-11D-229.1	−229.1	23.4	25.0	6.2	3.8	7.1	9.6	26.7	5.2	25.7
TD-11D-230.2	−230.2	19.9	21.6	5.9	3.2	8.0	8.4	25.5	3.7	23.3
TD-11D-231.8	−231.8	24.2	26.1	11.0	2.7	6.8	10.1	30.5	8.4	27.9
TD-11D-233.8	−233.8	23.1	25.1	4.0	3.9	5.6	9.6	23.1	3.7	22.8
TD-11D-235.2	−235.2	22.1	24.3	3.8	3.8	5.2	9.0	21.8	3.8	21.8
CG-13U-176.6	−176.6	19.1	21.9	7.7	3.7	5.1	4.9	21.3	7.5	21.1
CG-13U-178.6	−178.6	22.2	24.4	9.0	4.0	4.8	5.8	23.7	9.0	23.7
CG-13U-180.5	−180.5	25.3	25.2	7.5	3.7	6.8	7.7	25.7	7.3	25.5
CG-13U-184.5	−184.5	25.5	25.8	7.8	5.0	6.1	7.8	26.7	7.2	26.1
CG-13U-186.5	−186.5	22.3	22.9	8.7	4.7	9.3	6.5	29.1	6.7	27.1
CG-13U-191.6	−191.6	26.6	26.9	8.9	4.8	4.7	8.0	26.5	8.9	26.5
CG-13U-193.8	−193.8	23.9	24.5	8.4	4.4	7.0	7.2	27.0	7.5	26.1
CG-13U-182	−182	20.6	21.7	6.5	3.9	5.2	5.5	21.1	6.5	21.1
CG-13U-175.7	−175.7	25.0	25.3	8.7	4.3	4.5	6.4	23.9	8.7	23.9

https://doi.org/10.1346/CCMN.2018.064111 Published online by Cambridge University Press

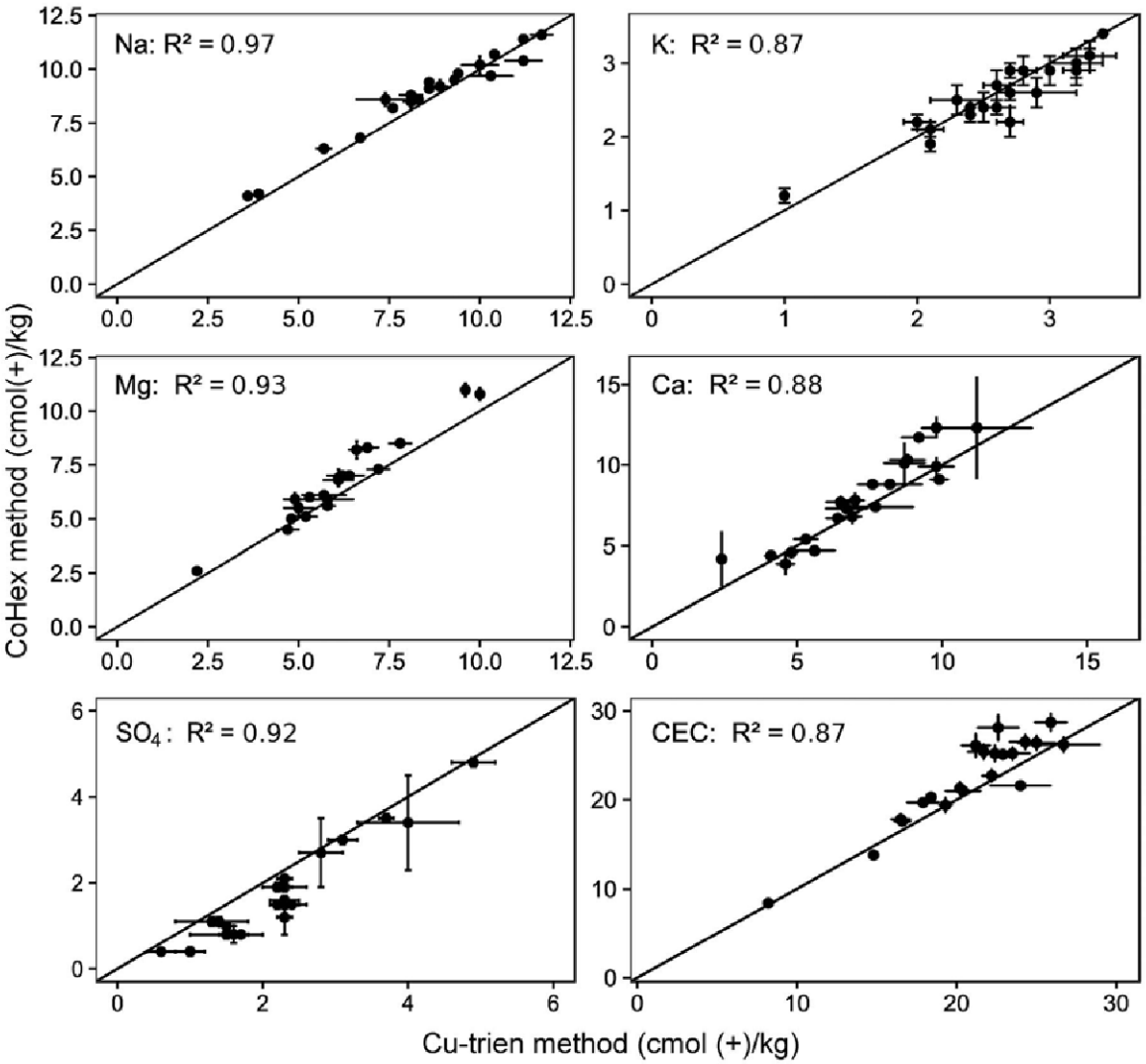

Figure 3. Comparison of the individual elements and the CEC determined by both the CoHex and Cu-trien methods for the main sample set. Standard deviations were based on two measurements per sample.

near vicinity of the HADES URF were discarded intentionally from the data set, because their composition is disturbed by the presence of the underground laboratory and related oxidation effects (De Craen *et al.*, 2008). In addition, the data from two piezometers containing an SO_4 concentration exceeding 0.10 mmol/L were not taken into account here as they were considered to have been altered significantly.

In accordance with De Craen *et al.* (2004a), who defined the Boom Clay pore water as a $NaHCO_3$-type water, the dominant cation was found to be Na, at an average concentration of 13.2 ± 2.5 mmol/L. Other major cations were K ($\bar{x}$ = 0.16 ± 0.02 mmol/L), Si ($\bar{x}$ = 0.18 ± 0.04 mmol/L), Ca ($\bar{x}$ = 0.05 ± 0.01 mmol/L), and Mg ($\bar{x}$ = 0.06 ± 0.01 mmol/L). The cation concentrations do not seem to show strong correlation, with the exception of Ca and Mg (R^2 = 0.75). The major anions present in the pore water were HCO_3 ($\bar{x}$ = 11.6 ± 2.1 wt.%), Cl ($\bar{x}$ = 0.56 ± 0.12 wt.%), and SO_4 ($\bar{x}$ = 0.02 ± 0.02 wt.%). The Cl and HCO_3 concentrations correlate strongly with the Na concentrations (R^2 = 0.96 and 0.84, respectively).

For the cations considered to be active in cation exchange processes, a depth plot is presented (Figure 4). In general, the concentrations of Ca, Mg, and K are quite stable throughout the Boom Clay. On the other hand, the Na concentration increases consistently with depth, from 232 mg/L in the uppermost piezometer filter (CG-13U-1) in the Boeretang Member, to as high as 337 mg/L in the lowermost piezometer filter (CG-13D-1) in the Terhagen Member. No piezometer is present in the lowermost Belsele-Waas Member.

Apart from the large-scale variations, an abrupt increase in most elemental concentrations is apparent at the base of the Putte Member at a depth of

https://doi.org/10.1346/CCMN.2018.064111 Published online by Cambridge University Press

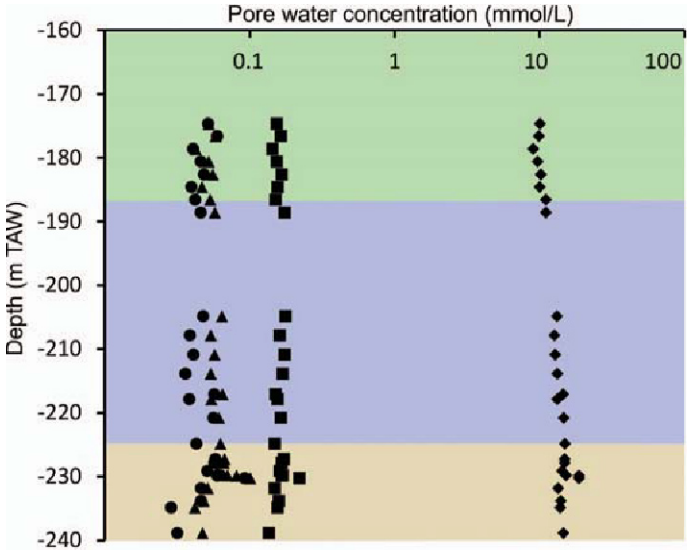

Figure 4. Concentrations of the major exchangeable cations in the pore water: Na (diamonds), K (squares), Ca (triangles), and Mg (circles). The color changes from top to bottom refer to the Boeretang Member, the Putte Member, and the Terhagen Member.

−230 mTAW. This peak is attributed to the presence of the so-called double band – a stratigraphic marker consisting of two very silt-rich layers. This double band is characterized by a sharp increase in hydraulic conductivity and apparent diffusion coefficient (HTO and iodide), parameters which were reported by Aertsens *et al.* (2004, 2005).

Mineralogical composition

The bulk-rock mineralogy of the main sample set (Table 5) is dominated by quartz ($\bar{x}$ = 36 ± 12 wt.%) and 2:1 clay minerals ($\bar{x}$ = 39 ± 11 wt.%). Secondary phases include K-feldspar ($\bar{x}$ = 7 ± 2 wt.%), plagioclase ($\bar{x}$ = 36 ± 12 wt.%), chlorite ($\bar{x}$ = 2 ± 1 wt.%), and kaolinite ($\bar{x}$ = 7 ± 3 wt.%). In five samples, located toward the top and bottom of the Boom Clay formation, glauconite was also identified as a minor component.

Oriented patterns of the Ca-saturated <2 μm fraction were modeled (Figure 5) to quantify the clay mineralogy. The proportion of 2:1 clay minerals in the bulk rock was split into proportions of smectite, illite, and mixed-layered illite-smectite using the information from the quantified clay mineralogy. On average, the bulk rock consists of 11 ± 3 wt.% smectite, 17 ± 5 wt.% mixed-layered illite-smectite, and 11 ± 4 wt.% illite. As the composition of the mixed layers was also quantified (on average 32 ± 2% smectitic layers), the total amount of smectitic and illitic layers in the bulk rock could be calculated for each sample (Table 6). The average amount of smectitic layers in the bulk rock is 17 ± 4 wt.%, while the amount of illitic layers is consistently larger, at 23 ± 8 wt.%.

DISCUSSION

Correction of exchangeable cation data

Systematic differences exist between the measured CEC and the sum of cations, with the sum being consistently greater than the CEC (Tables 2–4). As the measured CEC values were in the range of values found by Honty (2010) and Zeelmaekers *et al.* (2015), the sum of cations was assumed to be too high, rather than the CEC too low. The excess in the sum of cations can be attributed to two factors: on the one hand the dissolution of minerals unstable in the pH and redox environment created by the Cu-trien matrix, and on the other hand the presence of salts in the pore water.

The first process can be checked by examining the bulk-rock mineralogy. The only potentially unstable minerals present in the Boom Clay Formation are carbonate minerals, mainly represented by calcite, authigenic gypsum, and pyrite, which can be oxidized to form gypsum. The dissolution of calcite was suppressed by saturating the exchange complex with calcite prior to the experiments, although whether calcite dissolved during cation exchange or not was not confirmed. The dissolution of gypsum, resulting in an elevation of the sulfur and calcium concentrations, is a distinct possibility. As reported by Dohrmann and Kaufhold (2010), a reliable adjustment of the Ca occupancies in the case of gypsum dissolution is only possible by combining chemical (*i.e.* the Ca concentration) and mineralogical (the gypsum concentration) data. Adjusted Ca occupancies were calculated using sulfate concentrations from the ICP analyses for the entire extended sample set, while they were also calculated using gypsum concentrations from the XRD data of the

https://doi.org/10.1346/CCMN.2018.064111 Published online by Cambridge University Press

Table 5. Bulk-rock composition determined by combining quantitative bulk-rock data with clay-fraction data by splitting the proportion of 2:1 clays.

Sample	Qz	Kfs	Pl	Cal	Sd	Dol	Py	Gp	Ant	Ap	OM	Kln	Chl	Sme	Ilt-Sme	Ilt	Gl
ON-Mol-1-43b	48	6	7	0.9	0.4	0.9	0.9	0.3	2	0.2	1.0	5	4	8	7	5	4
ON-Mol-1-60b	43	11	3	0.7	0	0	1	0.2	1	0.2	1.4	5	2	10	12	10	0
ON-Mol-1-63b	39	12	3	0.3	0	0.4	1	0.6	1	0.2	1.9	5	4	10	13	9	0
ON-Mol-1-67b	32	7	3	0	0	0.3	2	0.2	0.8	0.2	2.3	7	4	12	18	13	0
ON-Mol-1-72b	19	8	1	0.9	0	0.4	0.5	0.4	2	0.2	1.2	12	2	13	20	19	0
ON-Mol-1-73b	25	4	0.6	0.4	0	0.5	1	0.1	1	0.2	1.7	9	3	12	23	19	0
ON-Mol-1-76b	29	5	3	0.8	0	0.2	4	0.5	0.8	0.2	4.8	6	0.4	10	23	13	0
PRACLAY	31	6	2	0.3	0	0.1	2	0.3	0.9	0.2	2.8	9	3	12	19	12	0
ON-Mol-1-78b	29	5	2	0.3	0	0.6	1	0.2	1	0.2	1.8	8	4	11	22	15	0
ON-Mol-1-82c11	30	6	3	0	0	0.1	2	0.2	2	0.2	3.1	10	3	10	20	11	0
ON-Mol-1-90c11	25	6	2	0	0	0.2	2	0.1	1	0.2	2.6	8	2	17	24	11	0
ON-Mol-1-98c1	41	6	2	0	0	0.3	1	0.1	0.2	0.1	1.6	6	4	11	18	8	0
ON-Mol-1-102a1	45	5	0.7	0	0	0	1	0.1	0.6	0.2	1.8	7	0.8	11	17	10	0
ON-Mol-1-103b	30	7	2	0	0	0	2	0.2	0.9	0.2	2.2	11	2	17	19	8	0
ON-Mol-1-108b	26	7	2	0.5	0	0.3	2	0.2	0	0.2	3.2	10	3	12	20	14	0
ON-Mol-1-115b	24	7	0.9	2	4	0.3	0.2	0.3	1	0.2	1.1	12	2	11	23	12	0
ON-Mol-1-119b	39	9	3	0	0.2	0.1	1	0.2	0.8	0.1	1.2	6	4	10	17	8	0
ON-Mol-1-125b	32	5	0.6	6	0	0.3	0.8	0	2	0.1	1.0	6	3	14	18	8	2
ON-Mol-1-130a2	46	10	3	0.2	0	0.2	0.4	0.3	0.5	0.1	1.0	6	1	13	12	5	2
ON-Mol-1-131b	43	7	3	0.9	0	0.4	0.7	0.2	1	0.1	1.0	5	0.4	12	13	11	2
ON-Mol-1-143b	71	7	6	0.6	0	0	0.3	0.1	0.5	0.1	0.4	0.9	0	4	4	2	3

Qz = Quartz, K-Fel = K-Feldspar, Pl = Plagioclase, Cal = Calcite, Sd = Siderite, Dol = Dolomite, Py = Pyrite, Gp = Gypsum, Ant = Anatase, Ap = Apatite, OM = Organic Matter, Kln = Kaolinite, Chl = Chlorite, Sme = Smectite, Ilt-Sme = Mixed-layered illite-smectite, Ilt = Illite, Gl = Glauconite. Results are expressed in wt.%. Deviations from 100 wt.% are due to rounding.

main sample set and the sample set of Zeelmaekers *et al.* (2015). In both methods, the sulfate/gypsum concentration was recalculated to cmol(+)/kg and subsequently subtracted from the Ca concentration to obtain an adjusted Ca occupancy. The adjusted Ca occupancies calculated using both methods are almost identical (R^2 = 0.92, Ca(gypsum) = 1.002Ca(sulfate)).

After adjustment, the sum of cations fitted closer to the CEC (Figures 6, 7). The remaining overshoot could be attributed to salts present in the pore water. As the Cl concentrations were not probed in the Cu-trien or CoHex solutions, an alternative method was attempted. The Cl concentrations measured in the piezometer filters were interpolated over the interval of the sample set, and those

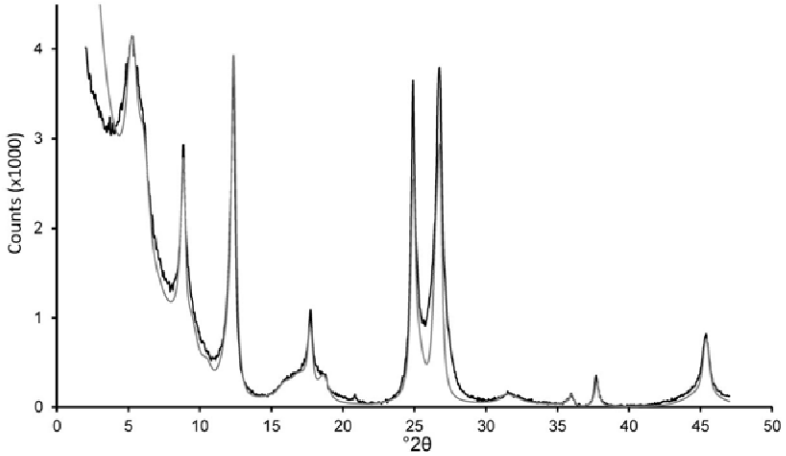

Figure 5. XRD pattern (black line) of the <2 μm fraction of a glycolated Boom Clay sample (ON-Mol-1-072). The gray line indicates the pattern as it was modeled in the *Sybilla* software.

https://doi.org/10.1346/CCMN.2018.064111 Published online by Cambridge University Press

Table 6. Total amount of smectitic and illitic layers in the bulk rock of the main sample set. All numbers are expressed in wt.%.

Sample	Smectitic	Illitic
ON-Mol-1-43b	10	10
ON-Mol-1-60b	13	18
ON-Mol-1-63b	14	18
ON-Mol-1-67b	18	25
ON-Mol-1-72b	19	34
ON-Mol-1-73b	19	35
ON-Mol-1-76b	17	30
PRACLAY	18	25
ON-Mol-1-78b	18	30
ON-Mol-1-82c11	16	25
ON-Mol-1-90c11	24	28
ON-Mol-1-98c1	17	21
ON-Mol-1-102a1	17	22
ON-Mol-1-103b	23	21
ON-Mol-1-108b	18	28
ON-Mol-1-115b	19	27
ON-Mol-1-119b	16	20
ON-Mol-1-125b	20	21
ON-Mol-1-130a2	17	13
ON-Mol-1-131b	16	19
ON-Mol-1-143b	6	4

concentrations were used as a proxy for the Na concentrations, as NaCl is the most common salt present in Boom Clay pore water (De Craen *et al.*, 2004a). The Cl inventory was then calculated using the following formula:

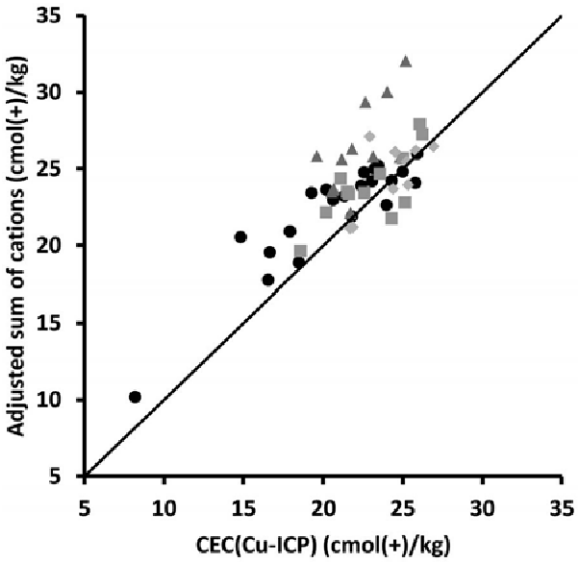

Figure 6. Comparison of the CEC(Cu-ICP) with the sum of exchangeable cations (Na, Mg, K, and Ca) after adjustment for the sulfate concentration. Circles indicate the main sample set, triangles the set of Zeelmaekers *et al*. (2015), squares the set of De Craen *et al.* (2004b), and diamonds the set of De Craen (2005).

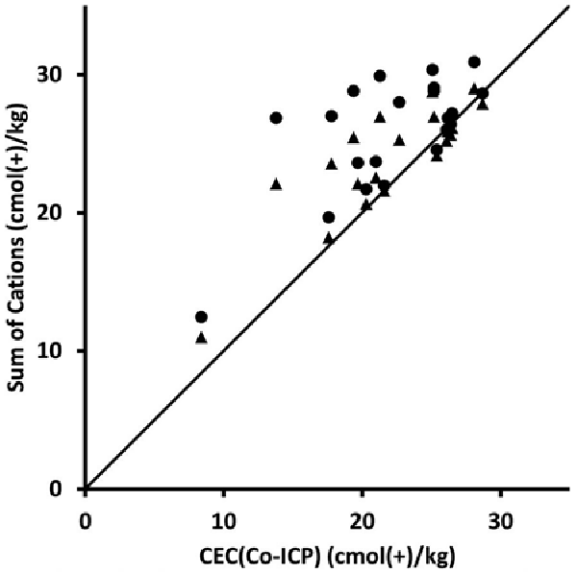

Figure 7. Comparison of the CEC(Co-ICP) with the sum of exchangeable cations (Na, Mg, K, and Ca) of the main sample set before (circles) and after (triangles) adjustment for the sulfate concentration.

$$\mathrm{Cl}\left(\frac{\mathrm{cmol(+)}}{\mathrm{kg}}\right) = \frac{\mathrm{Moisture\ (wt.\%)} \times \mathrm{Cl}\left(\frac{\mathrm{mg}}{\mathrm{L}}\right)}{10 \times M\left(\frac{\mathrm{g}}{\mathrm{mol}}\right) \times (100 - \mathrm{Moisture\ (wt.\%)})} \quad (1)$$

with M being the molar mass.

With an average moisture content of 20 ± 3 wt.% in the range of 0 to 110ºC, the average Cl inventory was determined at 0.013 ± 0.003 cmol(+)/kg. This value fits closely with the Cl concentration of 0.0145 ± 0.0035 cmol/L in Boom Clay water extracts reported by Baeyens *et al.* (1985). The calculated Cl inventory is negligible compared to the excess occupancies. The same approach can be applied to HCO_3, which is present in greater concentrations in the Boom Clay pore water. These calculations resulted in an average HCO_3 inventory of 0.28 ± 0.06 cmol(+)/kg, which was still too low to eliminate the overestimation of the sum of exchangeable cations. Significant salt contributions to the exchangeable cation population were, therefore, dismissed and the overestimation of the sum of exchangeable cations could not be reduced. Nevertheless, the excess was limited to 8% for the entire sample set for both the Cu-trien and CoHex methods.

The exchangeable cation population determined by the Cu-trien method was plotted on a ternary diagram (Figure 8) with Ca occupancies adjusted as described above. With a few exceptions, all samples were concentrated in a single region, an indication that the pore-water composition does not vary significantly throughout the Boom Clay stratigraphy. The average

https://doi.org/10.1346/CCMN.2018.064111 Published online by Cambridge University Press

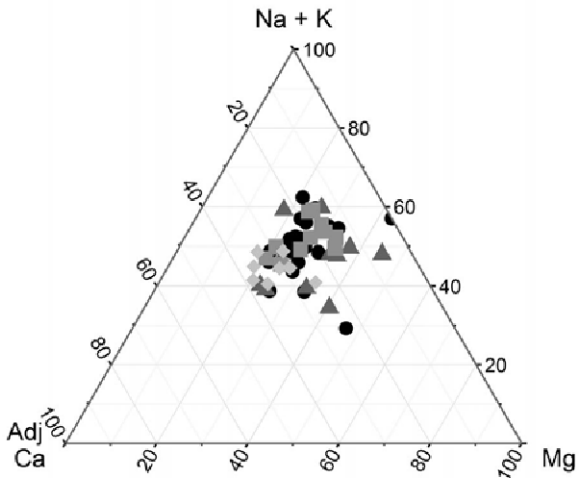

Figure 8. Exchangeable cation population of the complete sample set after adjustment for the dissolution of gypsum. Circles indicate the main sample set, triangles the set of Zeelmaekers *et al.* (2015), squares the set of De Craen *et al.* (2004b), and diamonds the set of De Craen (2005).

population consists of 24 ± 8% Ca, 28 ± 7% Mg, 35 ± 7% Na, and 13 ± 3% K. The exchangeable cation population measured by the CoHex method was similar to that of the Cu-trien method, with an average of 25 ± 7% Ca, 28 ± 7% Mg, 36 ± 7% Na, and 11 ± 1% K. Considering analytical scattering, the exchangeable cation population of both techniques was nearly identical.

CEC and mineralogy

As reported by Środoń (2009) and Zeelmaekers *et al.* (2015), the CEC can be used as an excellent proxy for the bulk-rock smectite content, as the CEC of an average charged smectite lies in the range of 103−110 cmol(+)/kg. The bulk-rock smectitic content may be calculated as 0.91 × CEC at a layer charge of 0.41 charge per half unit cell, according to Środoń (2009).

A strong positive correlation between the bulk-rock smectitic content and the CEC(Cu-ICP) is shown in Figure 9. The trend line is similar to that reported by Zeelmaekers *et al.* (2015), although the intercept with the vertical axis is slightly higher here. The greater intercept is mainly influenced by the data points in the 15−20 wt.% smectite range, the same range in which Zeelmaekers *et al.* (2015) reported a number of points deviating from the general trend. The higher-than-expected CEC value in this range could indicate non-smectitic contributions to the CEC. This hypothesis was advanced by Zeelmaekers *et al.* (2015), based on the positive-compared-to-zero intercept of pure smectite (Środoń, 2009). A number of explanations was put forward by those authors to explain this intercept. The first explanation was related to contributions by organic matter to the CEC. Evidence for this explanation was lacking in the present study, however, as no significant correlation (R^2 = 0.08) was found between the bulk-rock organic-matter content and the deviation from the trend calculated by Środoń (2009). A second explanation considers contributions from smectitic mineral layers in kaolinite-smectite mixed-mineral layers. On average, the main sample set consists of 3.7 ± 2.0 wt.% of kaolinite-smectite mixed-mineral layers. These mineral layers comprise 20 ± 1% of the smectitic mineral layers, amounting to an average increase of 1.5 ± 0.7 cmol(+)/kg for the total smectitic content in the bulk rock. Considering that the average difference with the trend described by Środoń (2009) is

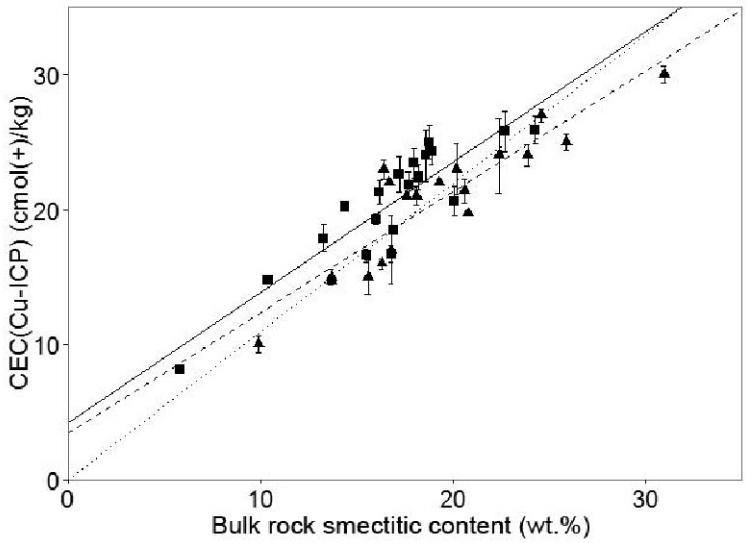

Figure 9. Comparison of the bulk-rock smectitic content with the CEC(Cu-ICP) for the main sample set (squares) and the data set presented by Zeelmaekers *et al.* (2015) (triangles). The dotted line indicates the trend presented by Środoń (2009), the solid black line is the trend based on the main sample set, and the dashed line is the trend based on the results of Zeelmaekers *et al.* (2015).

https://doi.org/10.1346/CCMN.2018.064111 Published online by Cambridge University Press

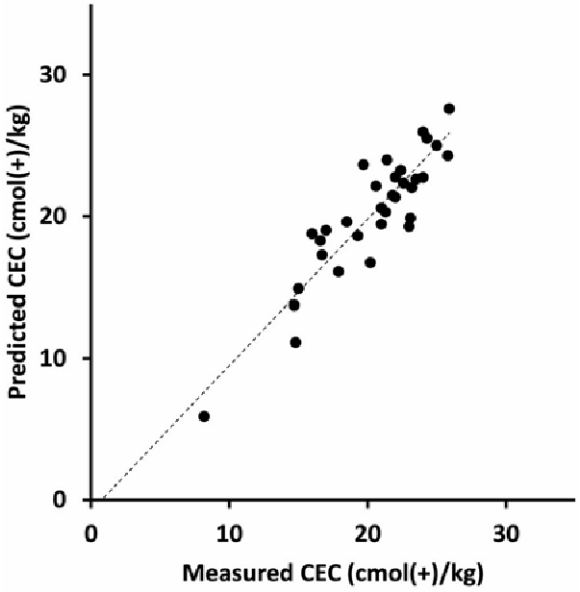

Figure 10. Comparison of the measured CEC values with CEC values modeled by incorporating the bulk-rock smectitic and illitic content. The correlation coefficient (R^2) of the dashed trend line is 0.81.

still 2 ± 1 cmol(+)/kg after correction, another mechanism must be at work. The mechanism could be provided by a third explanation offered by Zeelmaekers *et al.* (2015): illitic surfaces and edges contributing to the total CEC.

Although the contributions of illite cannot be proven directly based on the available data, the CEC of the main sample set and of the samples of Zeelmaekers *et al.* (2015) can be modeled using the bulk-rock smectitic and illitic content (Table 6). These parameters are multiplied by an estimate of the CEC of the smectitic and illitic components to obtain a prediction for the CEC of each sample. The root-mean-square error (RMSE) was subsequently minimized by varying the estimated CEC of the illitic and smectitic layers with an evolutionary algorithm. The best fit (R^2 = 0.81) was achieved (Figure 10) at an RMSE value of 1.91 cmol(+)/kg, with a sufficiently small intercept. The estimated CEC of the smectitic component is 80 cmol(+)/kg, while the estimated CEC of the illitic component is 30 cmol(+)/kg. The high estimated CEC of the illitic component indicates a significant contribution to the bulk-rock CEC, which would explain the deviation of the trend proposed by Środoń (2009).

Exchangeable cations and pore-water chemistry

As demonstrated above, the only cation to show any noteworthy trend throughout the Boom Clay is Na. The evolution of the Na concentrations is similar to the evolution of the HCO_3 concentrations, which implies that the Boom Clay pore water can be defined as a $NaHCO_3$-type water (Figure 11). A similar evolution is visible in the Cl concentrations, which show a high degree of correlation (R^2 = 0.96) to the Na concentrations. The Na occupancies, when plotted as a portion of the adjusted sum of exchangeable cations, also show an upward decreasing trend. Whether this trend is influenced by the current pore-water composition can only be elucidated when a sample-by-sample comparison is available. Because only a limited number of clay samples were taken at the same depth as the piezometer filters, the choice was made to interpolate the pore-water compositions using the inverse distance weighting (IDW) algorithm in one dimension.

When the interpolated Na concentration is compared with the Na occupancies at identical depths, a moderately positive correlation is evident (R^2 = 0.54) (Figure 12). The correlation coefficient is heavily influenced by one outlier with an interpolated Na concentration of 425 mg/L, the depth of which (−230.3 m TAW) tallies with the double band discussed above. Due to its deviant hydrological properties, the pore-water composition of the outlier is markedly different from that of its surroundings. Remarkably, these changes are not visible in the Na occupancies, which are in line with neighboring observations. A plausible explanation for this discrepancy would be that different diffusion coefficients operate in the pore space and in the clay interlayers, the latter being less affected by the ambient hydraulic conditions. Alternatively, a relative increase in the ionic strength can change the properties of the double layer of clay minerals, which affects the diffusion of cations near the clay surface, but not necessarily in the clay interlayers. Whatever the reason behind the relatively constant cation occupancies in this specific layer, this observation deserves attention in future research. If the outlier is removed, the correlation coefficient improves significantly (R^2 = 0.61). The observed trend in terms of both pore water and occupancies is caused by the same process. The process is probably a progressive mixing of originally marine pore waters with meteoric infiltration. As a shallow-marine deposit, the Boom Clay's pore-water composition was originally saline, which is why the Na concentration is relatively high, especially toward the bottom of the formation. Around 2 My ago, meteoric waters started infiltrating through the silt-rich top of the formation, leading to a progressive decrease in the Na and Cl concentrations in the pore waters through dilution (Mazurek *et al.*, 2009, 2011).

According to De Craen *et al.* (2004a), infiltrating meteoric water increases locally the Ca concentration in the pore water and promotes the exchange of the dominant Na by Ca on clay surfaces. A decrease in the Ca occupancies is visible (24% Ca at −163 m TAW to 15% Ca at −222 m TAW), but numerous spikes are seen. A meteoric Ca contribution is unlikely, therefore, to be significant or overprinted by the dissolution of Ca-bearing mineral phases within the Boom Clay. Similarly, no consistent trend was observed in the Ca concentrations in the pore water.

https://doi.org/10.1346/CCMN.2018.064111 Published online by Cambridge University Press

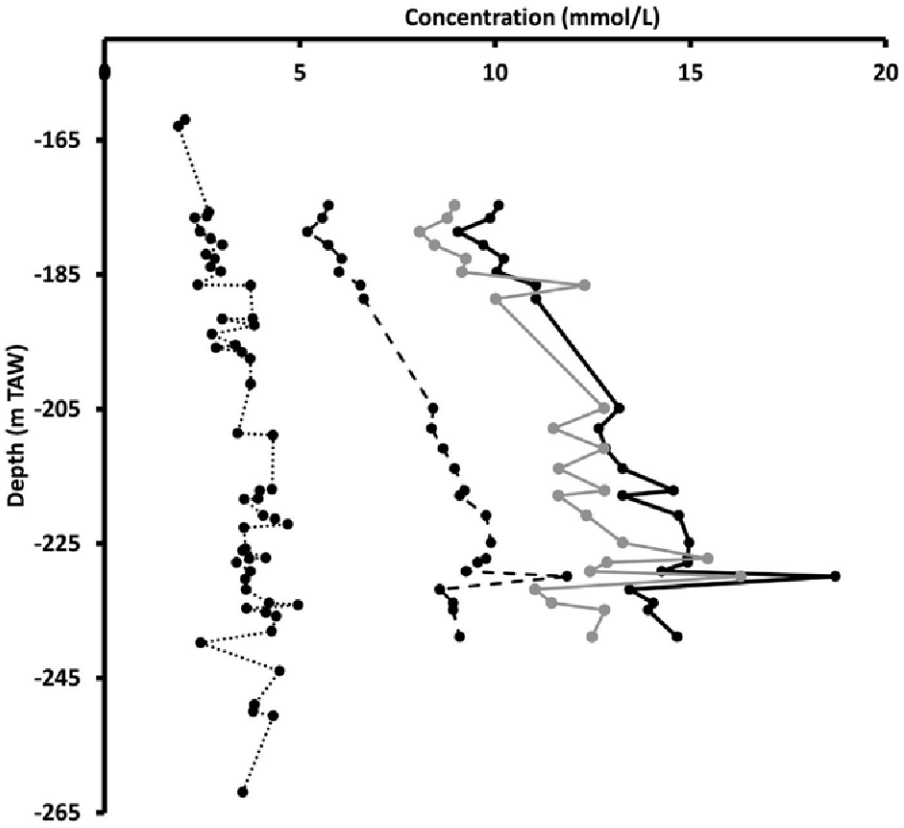

Figure 11. Evolution of the concentration of a number of elements in the Boom Clay pore water. Na concentrations are indicated with a solid black line and HCO_3 concentrations with a solid gray line. Cl concentrations (dashed line) were scaled by a factor of 15 to allow comparison with Na and Cl. The proportions of Na in the exchangeable cation population (dotted line) were scaled by a factor of 10 to allow comparison.

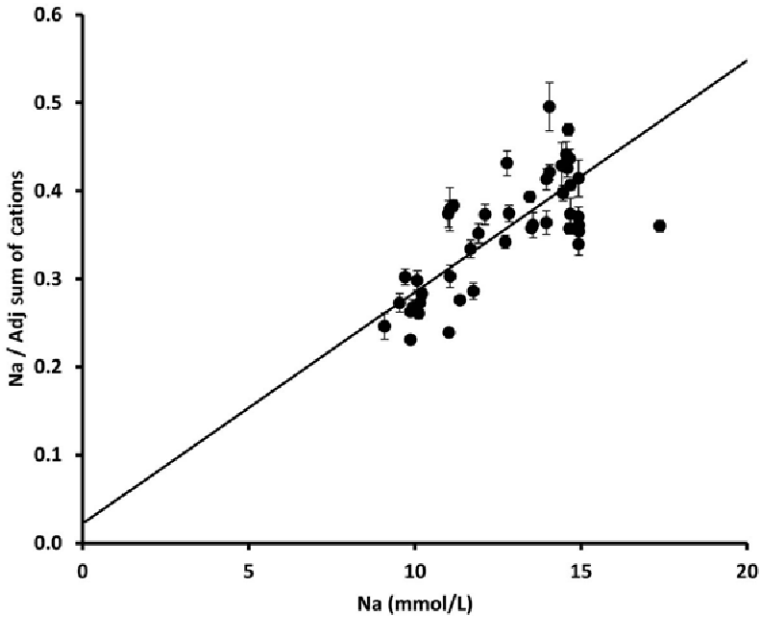

Figure 12. Scatter plot of the interpolated pore-water concentrations and the proportion of Na in the exchangeable cation population. After exclusion of the sample from the double band, the correlation coefficient increased from $R^2 = 0.54$ to $R^2 = 0.61$.

https://doi.org/10.1346/CCMN.2018.064111 Published online by Cambridge University Press

Selectivity coefficients

The availability of pore-water compositions and exchangeable cation populations allow for the calculation of selectivity coefficients for the major cations. Selectivity coefficients are calculated separately for each of the main exchangeable cation pairs. In the case of a K-Na exchange, the selectivity coefficient can be expressed as:

$$K_c(\text{K-Na}) = \frac{[> X : \text{K}]\ \{\text{Na}^+\}}{[> X : \text{Na}]\ \{\text{K}^+\}} = \frac{N_\text{K}\{\text{Na}^+\}}{N_\text{Na}\{\text{K}^+\}} \quad (2)$$

In this equation [>*X*:K^+] and [>*X*:Na^+] express the potassium and sodium exchange complexes on the surface of the clay, while {Na^+} and {K^+} are the activities in the aqueous phase (De Craen *et al.*, 2004a). Following the Gaines-Thomas convention, the exchange complexes are expressed as equivalent fractions (N_{Na} and N_K) of the total exchange capacity (Gaines Jr and Thomas, 1953).

A set of selectivity coefficients based on some batch data obtained from drilling cores was reported by Baeyens *et al.* (1985) (Table 7). Those authors excluded exchangeable Ca, arguing that the pore-water content of Ca can be attributed exclusively to calcite. This claim was questioned by De Craen *et al.* (2004a) as the variation of major cations observed cannot be explained without the mechanism of Ca exchange. The measurement of exchangeable Ca in the current study, even after saturation of the exchange solution with calcite, confirms that, although the pore-water concentration of Ca might be controlled by the solubility of calcite, exchangeable Ca still exists. In addition, an exchangeable cation population, including exchangeable Ca, was determined by Griffault *et al.* (1996). Those data were taken into consideration by De Craen *et al.* (2004a) in the determination of the selectivity coefficients (Table 7).

The pore-water concentrations of the major cations (Na, Mg, K, and Ca) were interpolated using the same approach as described in the previous section to obtain pore-water compositions at depths identical to those of the samples used for CEC analysis. Samples above and below, respectively, the highest and lowest measured pore-water filter were excluded, as interpolation would not make sense here. In total, 45 sets of selectivity coefficients could be calculated in the interval of −175.70 to −238.00 m TAW. The selectivity coefficients (Figure 13) exhibited a range of values, with K_c(K-Na) being systematically larger than K_c(Ca-Na) and K_c(Mg-Na). The coefficients calculated by De Craen *et al.* (2004a) can be located on the lower end of each range, which can be attributed to the fact that the sum of exchangeable cations of the sample used in their calculations is 18.5 cmol(+)/kg, which would put it on the low end of the values determined in the present study.

Comparison with similar projects

The data in the present study can be compared with those of similar studies into clay host rocks for nuclear waste repositories, most notably the Opalinus Clay in Switzerland and the Callovo-Oxfordian Clay in France.

Most studies of the Opalinus Clay use Ni-ethylenediamine as the exchange complex (Bradbury and Baeyens, 1998; Pearson *et al.*, 2002). One study, by Pearson *et al.* (2002), discussed variations throughout the Opalinus Clay in the Mont Terri rock laboratory. The CEC of nine samples was found to vary from 8.4 cmol(+)/kg to 17.1 cmol(+)/kg. Noteworthy is that two samples were also measured with CoHex as the exchange complex, which resulted in significantly greater CEC values. The exchangeable cation populations of the nine samples measured with Ni-ethylenediamine (Table 8) contain less K and Mg, but more Ca and Na than the Boom Clay samples.

The CEC of the Callovo-Oxfordian (COX) Clay has been determined for a number of samples by numerous authors (Gaucher *et al.*, 2006; Klinkenberg *et al.*, 2009; Dohrmann *et al.*, 2012; Jacquier *et al.*, 2013) and varied significantly due to the presence of carbonate-rich horizons. An average value of 17.4 ± 6.1 cmol(+)/kg was reported by Gaucher *et al.* (2006). The exchangeable cation population (Table 8) reported by the same authors (sample size and exchange complex were not reported) was dominated by Ca and containing proportionally less Na than the Boom Clay samples.

Table 7. Overview of the selectivity coefficients (K_c) of the Boom Clay and the exchangeable cation population data (N) from which they were calculated.

Parameter	Baeyens *et al.* (1985)	Griffault *et al.* (1996) and De Craen *et al.* (2004a)	Current study
N_{Na}	0.37	0.47	0.35 ± 0.07
N_K	0.16	0.12	0.13 ± 0.03
N_{Ca}	excluded	0.20	0.24 ± 0.08
N_{Mg}	0.48	0.20	0.28 ± 0.07
K_c (K-Na)	10	21.28	30.24 ± 8.09
K_c (Mg-Na)	3.8	4.76	8.60 ± 2.71
K_c (Ca-Na)	excluded	6.96	9.16 ± 3.93

https://doi.org/10.1346/CCMN.2018.064111 Published online by Cambridge University Press

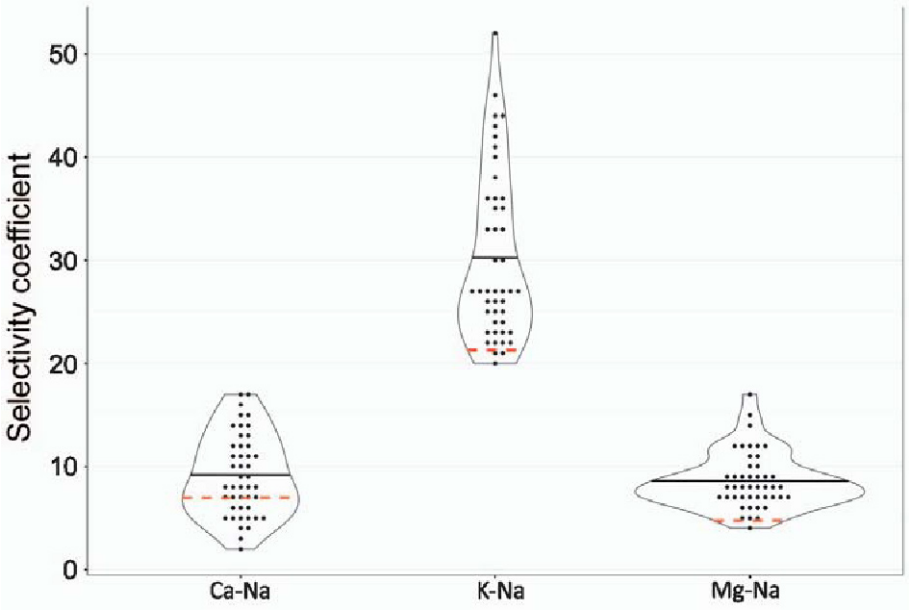

Figure 13. Violin plot comparing the selectivity coefficients calculated for 45 samples. The average coefficient for each cation pair is indicated with a full bar, while the selectivity coefficients calculated by De Craen *et al.* (2004a) are indicated with a dashed line.

CONCLUSIONS

For the first time the CEC of the Boom Clay Formation was probed systematically, indicating a CEC varying between 8.2 and 26.9 cmol(+)/kg, with an average of 22.2 ± 3.3 cmol(+)/kg. Within this range, significant variations throughout the Boom Clay were observed, related to variations in clay mineral content. In combination with the exchangeable cation data, this forms an elaborate database, with a size exceeding previously published data. A comparison of the Cu-trien method with the CoHex method proved the quality of the data, although the determination of the sulfate concentrations is probably more accurate with the CoHex method. The total CEC is correlated with the bulk-rock smectitic content, whereas the exchangeable cation population reflects *in situ* pore-water compositions. The CEC values and the exchangeable cation data were used to calculate a range of selectivity coefficients, indicating that these coefficients are not constant throughout the Boom Clay. In addition, the exchangeable cation data provided independent proof of the meteoric mixing theory put forward by Mazurek *et al.* (2009).

ACKNOWLEDGMENTS

The authors thank ONDRAF/NIRAS, the Belgian Agency for Radioactive Waste and Fissile Materials for providing the clay cores on which the study was carried out. The views presented by the authors do not necessarily represent the views of ONDRAF/NIRAS. Dr Nancy Weyns and Dr Elvira Vassilieva are thanked for the XRD and ICP analyses, respectively, conducted at the KU Leuven, while Maxime Ferreol is thanked for his assistance with the CEC analyses of the extended sample set.

REFERENCES

Aertsens, M., Wemaere, I., and Wouters, L. (2004) Spatial variability of transport parameters in the Boom Clay. *Applied Clay Science*, **26**, 37–45.

Aertsens M., Dierckx, A., Put M., Moors H., Janssen K., van Ravestyn L., Van Gompel M., Van Gompel M., and De Cannière P. (2005) Determination of the hydraulic conductivity, ηr and the apparent diffusion coefficient on Ieper clay and Boom Clay cores from the Doel-1 and Doel-2b drillings. *Final report to NIRAS/ONDRAF on Tasks 2.71*

Table 8. Exchangeable cation populations of the three clay formations discussed, expressed as a percentage of the sum of cations. For the Boom Clay, the cation population after adjustment for gypsum dissolution was used.

Cation	Boom Clay (range)	Opalinus (range)	Boom Clay (average)	COX (average)
Na	19–50	31–49	35 ± 7	18 ± 2
K	7–19	5–10	13 ± 3	8 ± 1
Ca	0–40	17–33	24 ± 8	45 ± 2
Mg	18–47	16–31	28 ± 7	25 ± 2
Sr	NA	1–4	NA	4

https://doi.org/10.1346/CCMN.2018.064111 Published online by Cambridge University Press

and 2.73 covering the period 1998–1999, SCK·CEN-R-3589, SCK·CEN, Mol, Belgium., 285 pp.

Ammann, L., Bergaya, F., and Lagaly, G. (2005) Determination of the cation exchange capacity of clays with copper complexes revisited. *Clay Minerals*, **40**, 441–453.

Bache, B.W. (1976) The measurement of cation exchange capacity of soils. *Journal of the Science of Food and Agriculture*, **27**, 273–280.

Baeyens, B., Maes, A., Cremers, A., and Henrion, P.N. (1985) In situ physico-chemical characterization of Boom Clay. *Radioactive Waste Management and the Nuclear Fuel Cycle*, **6**, 391–408.

Bastiaens, W., Van Cotthem, A., and Voorspoels, T. (2008) Design and realisation of the PRACLAY experimental gallery. Pp. 233–230 in: *Proceedings of the Congrès international de Monaco*, October 2008.

Beaucaire, C., Pitsch, H., Toulhoat, P., Motellier, S., and Louvat, D. (2000) Regional fluid characterisation and modelling of water-rock equilibria in the Boom Clay formation and in the Rupelian aquifer at Mol, Belgium. *Applied Geochemistry*, **15**, 667–686.

Bergaya, F. and Vayer, M. (1997) CEC of clays: Measurement by adsorption of a copper ethylenediamine complex. *Applied Clay Science*, **12**, 275–280.

Bradbury, M.H. and Baeyens, B. (1998) A physicochemical characterisation and geochemical modelling approach for determining porewater chemistries in argillaceous rocks. *Geochimica et Cosmochimica Acta*, **62**, 783–795.

Ciesielski, H., Sterckeman, T., Santerne, M., and Willery, J. (1997) A comparison between three methods for the determination of cation exchange capacity and exchangeable cations in soils. *Agronomie*, **17**, 9–16.

De Craen, M. (2005) *Geochemical characterisation of specific Boom Clay intervals*. SCK·CEN report R-4080, Mol, Belgium.

De Craen, M. and Mijnendonckx, K. (2017) *Boom Clay pore water chemistry around Hades: Reporting of the sampling and analyses performed in 2017*. Report 17/MDC/N-45,SCK-CEN, Mol, Belgium.

De Craen, M., Wang, L., Van Geet, M., and Moors, H. (2004a) *Geochemistry of Boom Clay pore water at the Mol site*. SCK·CEN scientific report BLG-990. Waste & Disposal Department SCK·CEN (Mol, Belgium).

De Craen, M., Van Geet, M., Honty, M., Weetjens, E., and Sillen, X. (2008) Extent of oxidation in Boom Clay as a result of excavation and ventilation of the Hades URF: Experimental and modelling assessments. *Physics and Chemistry of the Earth*, **33**, S350–S362.

De Craen, M., Wang, L., and Weetjens, E. (2004b) *Natural evidence on the long-term behaviour of trace elements and radionuclides in the Boom Clay*. Internal report R-3926, SCK·CEN, Mol, Belgium.

Deniau, I., Devol-Brown, I., Derenne, S., Behar, F., and Largeau, C. (2008) Comparison of the bulk geochemical features and thermal reactivity of kerogens from Mol (Boom Clay), Bure (Callovo–Oxfordian argillite) and Tournemire (Toarcian shales) underground research laboratories. *Science of the Total Environment*, **389**, 475–485.

Dohrmann, R. (2006) Cation exchange capacity methodology I: An efficient model for the detection of incorrect cation exchange capacity and exchangeable cation results. *Applied Clay Science*, **34**, 31–37.

Dohrmann, R. and Kaufhold, S. (2009) Three new, quick CEC methods for determining the amounts of exchangeable calcium cations in calcareous clays. *Clays and Clay Minerals*, **57**, 338–352.

Dohrmann, R. and Kaufhold, S. (2010) Determination of exchangeable calcium of calcareous and gypsiferous bentonites. *Clays and Clay Minerals*, **58**, 79–88.

Dohrmann, R., Kaufhold, S., and Lundqvist, B. (2013) The role of clays for safe storage of nuclear waste. Pp. 677–710 in: *Handbook of Clay Science* (F. Bergaya and G. Lagaly, editors). Developments in Clay Science, **5**, Elsevier, Amsterdam.

Dohrmann, R., Genske, D., Karnland, O., Kaufhold, S., Kiviranta, L., Olsson, S., Plötze, M., Sandén, T., Sellin, P., Svensson, D., and Valter, M. (2012) Interlaboratory CEC and exchangeable cation study of bentonite buffer materials: I. Cu(II)-triethylenetetramine method. *Clays and Clay Minerals*, **60**, 162–175.

Fernandez, A., Melon, A., Sanchez, D., Gaucher, E., Tournassat, C., Altmann, S., Vinsot, A., Maes, N., De Craen, M., Leupin, O., Wersin, P., and Astudillo, J. (2010) Study of different argillaceous formations performed in the context of the FUNMIG project (ENRESA-05/2009), Spain.

Gaines Jr, G.L. and Thomas, H.C. (1953) Adsorption studies on clay minerals. Ii. A formulation of the thermodynamics of exchange adsorption. *The Journal of Chemical Physics*, **21**, 714–718.

Gaucher, É.C., Blanc, P., Bardot, F., Braibant, G., Buschaert, S., Crouzet, C., Gautier, A., Girard, J.-P., Jacquot, E., and Lassin, A. (2006) Modelling the porewater chemistry of the Callovian–Oxfordian formation at a regional scale. *Comptes Rendus Geoscience*, **338**, 917–930.

Griffault, L., Merceron, T., Mossmann, J., Neerdael, B., De Cannière, P., Beaucaire, C., Daumas, S., Bianchi, A., and Christen, R. (1996) *Project Archimède-Argile. Acquisition et régulation de la chimie des eaux en milieu argileux pour le projet de stockage de déchets radioactifs en formation géologique*. Rapport final, International Workshop, Hydraulic and Hydrochemical characterisation of argillaceous rocks; 1994; Nottingham, UK. OECD Documents, pp. 105–118,

Hadi, J., Tournassat, C., and Lerouge, C. (2016) Pitfalls in using the hexaamminecobalt method for cation exchange capacity measurements on clay minerals and clay-rocks: Redox interferences between the cationic dye and the sample. *Applied Clay Science*, **119**, 393–400.

Honty, M. (2010) CEC of the Boom Clay – a review. SCK·CEN-ER-58, Mol, Belgium, 27 pp.

ISO-23470 (2007) Soil quality – determination of effective cation exchange capacity (cec) and exchangeable cations using a hexamminecobalt trichloride solution. https://www.iso.org/standard/36879.html.

Jackson, M.L. (1975) *Soil Chemical Analysis - Advanced Course*. Second edition. Published by the author, Madison, Wisconsin, USA.

Jacquier, P., Hainos, D., Robinet, J., Herbette, M., Grenut, B., Bouchet, A., and Ferry, C. (2013) The influence of mineral variability of Callovo-Oxfordian clay rocks on radionuclide transfer properties. *Applied Clay Science*, **83**, 129–136.

Klinkenberg, M., Kaufhold, S., Dohrmann, R., and Siegesmund, S. (2009) Influence of carbonate microfabrics on the failure strength of claystones. *Engineering Geology*, **107**, 42–54.

Maes, A., Vancluysen, J., and Bruggeman, C. (2003) Influence of oxidation on the cs cation exchange capacity of Boom Clay. *Unpublished report of the Catholic University of Leuven, Faculty of Bioscience Engineering, Centre for Surface Chemistry and Catalysis*, 16.

Mazurek, M., Alt-Epping, P., Gimi, T., Niklaus, W., Bath, A., and Gimmi, T. (2009) Natural tracer profiles across argillaceous formations: The CLAYTRAC project.

Mazurek, M., Alt-Epping, P., Bath, A., Gimmi, T., Waber, H.N., Buschaert, S., De Cannière, P., De Craen, M., Gautschi, A., and Savoye, S. (2011) Natural tracer profiles across argillaceous formations. *Applied Geochemistry*, **26**,

https://doi.org/10.1346/CCMN.2018.064111 Published online by Cambridge University Press

1035–1064.

Meier, L.P. and Kahr, G. (1999) Determination of the cation exchange capacity (CEC) of clay minerals using the complexes of copper (II) ion with triethylenetetramine and tetraethylenepentamine. *Clays and Clay Minerals*, **47**, 386–388.

Pearson, F., Arcos, D., Bath, A., Boisson, J., Fernández, A., Gäbler, H., Gaucher, E., Gautschi, A., Griffault, L., and Hernán, P. (2002) Geochemical program of the Mont Terri project: Summary of results and conclusions. Proceedings of the *1st International. Conference on Clays in Natural and Engineered Barriers for Radioactive Waste Confinement*, Reims, France.

Snellings, R., Machiels, L., Mertens, G., and Elsen, J. (2010) Rietveld refinement strategy for quantitative phase analysis of partially amorphous zeolitized tuffaceous rocks. *Geologica Belgica*, 183–196.

Środoń, J. (2009) Quantification of illite and smectite and their layer charges in sandstones and shales from shallow burial depth. *Clay Minerals*, **44**, 421–434.

Środoń, J. and McCarty, D.K. (2008) Surface area and layer charge of smectite from CEC and EGME/H_2O-retention measurements. *Clays and Clay Minerals*, **56**, 155–174.

Zeelmaekers, E., Honty, M., Derkowski, A., Środoń, J., De Craen, M., Vandenberghe, N., Adriaens, R., Ufer, K., and Wouters, L. (2015) Qualitative and quantitative mineralogical composition of the Rupelian Boom Clay in Belgium. *Clay Minerals*, **50**, 249–272.

(*Received 19 March 2018; revised 31 August 2018; Ms. 1274; AE: R. Kukkadapu*)